NANO LETTERS

pubs.acs.org/NanoLett

Black Ge Based on Crystalline/Amorphous Core/Shell Nanoneedle Arrays

Yu-Lun Chueh,[†,§,||,#] Zhiyong Fan,[†,§,||] Kuniharu Takei,[†,§,||] Hyunhyub Ko,[†,§,||] Rehan Kapadia,[†,§,||] Asghar A. Rathore,[†,§,||] Nate Miller,[‡,||] Kyoungsik Yu,[†,§] Ming Wu,[†,§] E. E. Haller,[‡,||] and Ali Javey[†,§,||,*]

[†]Department of Electrical Engineering and Computer Sciences, [‡]Department of Materials Science and Engineering, [§]Berkeley Sensor and Actuator Center, University of California at Berkeley, Berkeley, California 94720, [||]Materials Sciences Division, Lawrence Berkeley National Laboratory, Berkeley, California 94720, and [#]Current address: Department of Materials Science and Engineering, National Tsing Hua University, 101 sec 2, Kuang-Fu Road, Hsinchu 30013, Taiwan, ROC

ABSTRACT Direct growth of black Ge on low-temperature substrates, including plastics and rubber is reported. The material is based on highly dense, crystalline/amorphous core/shell Ge nanoneedle arrays with ultrasharp tips (~4 nm) enabled by the Ni catalyzed vapor−solid−solid growth process. Ge nanoneedle arrays exhibit remarkable optical properties. Specifically, minimal optical reflectance (<1%) is observed, even for high angles of incidence (~75°) and for relatively short nanoneedle lengths (~1 μm). Furthermore, the material exhibits high optical absorption efficiency with an effective band gap of ~1 eV. The reported black Ge could potentially have important practical implications for efficient photovoltaic and photodetector applications on nonconventional substrates.

KEYWORDS Black germanium, nanowires, nanoneedles, antireflective coating, thin absorbers

To achieve efficient absorption of light, exploration of novel three-dimensional (3D) structures with relevant material systems is essential. For instance, 3D micro/nanostructures have been shown to reduce light reflection while enhancing the absorption efficiency.[1] Vertical cone-shape pillars are attractive in that regard due to the gradual reduction of the effective refractive index of the material from the bottom to the top.[2] On the basis of this concept, black Si has been demonstrated in the past by utilizing various processes, including femto-second laser bombardment or patterned etching of the surface of bulk silicon and thin film (TF) substrates.[3] Black Si has been widely explored for photovoltaic and photodiode applications. Because of its smaller bandgap and unique optical properties, Ge planar and nonplanar structures have also been widely studied for infrared photodetector and photodiode applications.[4] Here, we report the direct synthesis of black Ge on a wide range of substrates, including glass, plastics, and rubbers using a low-temperature process. The reported black Ge consists of quasi-vertical crystalline/amorphous core/shell Ge nanoneedle (NN) arrays grown by Ni-catalyzed chemical vapor deposition process. The structures exhibit minimal reflectance even at large angles of incidence with an effective band gap of ~1 eV.

To grow Ge NNs, a thin film of Ni (~0.5 nm thick) was thermally evaporated on the substrate, followed by the growth at a sample temperature of 270−320 °C and a pressure of 1.8−280 Torr with GeH_4 (12 sccm, 10% balanced in H_2) used as the precursor gas. A representative transmission electron microscope (TEM) image of a Ge NN grown by this process is shown in Figure 1a, depicting the tapered feature with the tip and base diameters of ~4 and 70 nm, respectively. The high resolution TEM (HRTEM) image of the NN tip highlights a dome shaped catalyst with an atomic composition of 1:1, Ni:Ge from energy dispersive spectroscopy (EDS) (Supporting Information, Figure S1). The presence of the NiGe catalyst at the tip suggests that the growth mechanism is via either the vapor−liquid−solid

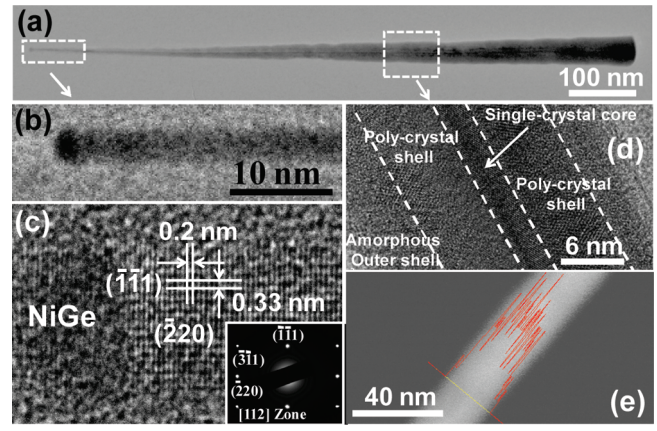

FIGURE 1. Ultrasharp Ge NNs. (a,b) TEM images of the Ge NNs. (c) HRTEM image of the nanoneedle tip, showing the NiGe catalytic seed. Inset shows the diffraction pattern with [110] growth direction. (d) HRTEM image from midsection of a NN where the single crystalline Ge core with polycrystalline and amorphous Ge shells are distinctly observed. (e) The EDS line profile reveals that the NN structure is pure Ge.

* To whom correspondence should be addressed. E-mail: ajavey@eecs.berkeley.edu.
Received for review: 10/9/2009
Published on Web: 12/30/2009

DOI: 10.1021/nl903366z | *Nano Lett.* **2010,** *10,* 520-523

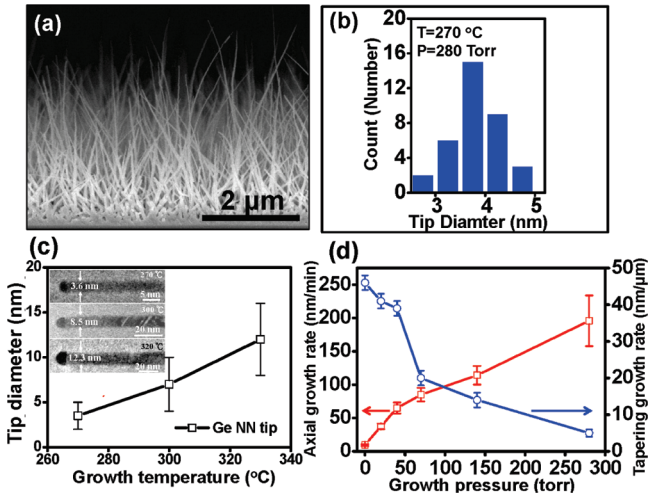

FIGURE 2. (a) SEM image of Ge NN arrays grown on a Si/SiO_2 substrate at 270 °C with pressure of 270 Torr. (b) Histogram of the tip diameter of Ge NNs grown at 270 °C. (c) The average tip diameter as a function of growth temperature. The inset shows representative TEM images of NNs grown at different temperatures. (d) The axial growth rate and tapering rate of Ge NNs at 280 °C as a function of growth pressure.

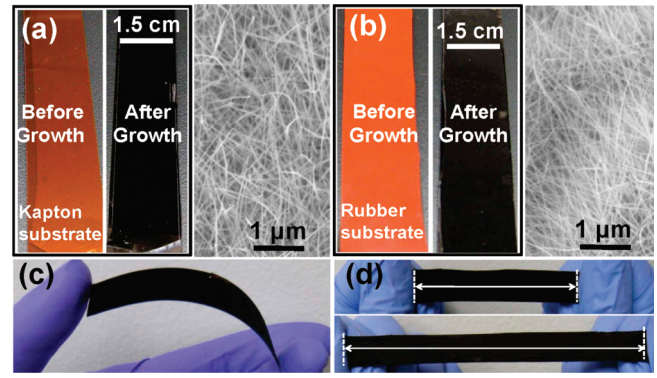

FIGURE 3. Direct growth of Ge NNs on deformable substrates. Optical and SEM images of Ge NNs grown on (a) flexible Kapton and (b) high-temperature rubber substrates. (c,d) The optical images of a bent Kapton substrate and stretched rubber with the Ge NNs grown on the surface. Notably, the substrates exhibit a visually black appearance.

(VLS)[5] or the vapor−solid−solid (VSS)[6] process. However, the growth temperature of 270−320 °C used in the present study is far below the eutectic temperature of the NiGe system (763 °C), suggesting that the growth of the NNs is most likely via the VSS mechanism.[7] The HRTEM analysis clearly shows that the NNs consist of three layers, namely, amorphous outer shell, polycrystalline inner shell, and an ultrathin single crystalline core (Figure 1d). The growth direction of the NN core is mainly along [110] (Figure 1c). The EDS elemental profile indicates that the entire structure is pure Ge (Figure 1e). This is also consistent with X-ray diffraction (XRD) analysis showing three main peaks, (111), (220), and (311) as depicted in Supporting Information, Figure S2. The formation of the shells we speculate is due to the lateral deposition of Ge atoms along the surface, resulting in the vapor−solid (VS) growth. Beyond a critical thickness of 5−10 nm, the shell becomes amorphous due to the lack of thermal energy for perfect epitaxial deposition.[8]

A scanning electron microscopy (SEM) image of a Ge NN array is shown in Figure 2a, depicting the quasi-vertical orientation of the NNs arising from the steric interactions of the highly dense array (~40 NNs/μm^2). The average tip diameter of the grown NNs is ~4 nm as analyzed by TEM (Figure 2b). The ultrasharp tip, thinner than the smallest diameter Ge NWs grown by Au nanoparticles, is attributed both to the size of the Ni nanoparticles formed from thin film evaporation, and the minimal coalescence during the growth.[9] To explore the detailed growth mechanism of Ge NNs, different growth temperatures and pressures were systematically explored. As the growth temperature is increased from 270 to 320 °C at a fixed growth pressure of 280 Torr, the tip diameter monotonically increases from ~4 to 13 nm (Figure 2c). The increased tip diameter with growth temperature is most likely due to the formation of larger Ni metal nanoparticle catalysts at higher temperatures prior to the initiation of the growth. However, Ge NNs are not grown as the growth temperature is reduced below ~260 °C, arising from the lack of reactivity of germane precursor and/or Ni catalytic seeds at such low temperatures. In addition, by increasing the growth pressure from 1.3 to 280 Torr at a fixed growth temperature of 270 °C, the axial growth rate is increased from ~10 to 200 nm/min (Figure 2d) due to the increased partial pressure of germane and higher incorporation rate of Ge atoms into the NiGe catalytic seeds. Meanwhile, the tapering rate, defined as the radial deposition rate over the axial growth rate decreases as the pressure is increased (Figure 2d). This can be explained by the phase diagram of the NiGe system that favors the VSS/VLS growth processes over noncatalytic radial deposition at higher pressures and lower temperatures. A similar trend was previously observed and reported for Au-catalyzed Si nanowires.[10]

The low-temperature growth process enables the direct synthesis of Ge NN arrays on a wide range of substrates, including flexible Kapton and stretchable rubber substrates (Figure 3a,b). The grown NNs are highly uniform over large areas. The ability to directly grow highly dense Ge NN arrays with unique optical properties on deformable substrates could potentially enable the exploration of a wide range of novel optoelectronic applications. Notably, the grown Ge NN arrays exhibit a black visual appearance (Figure 3a,b), despite the relatively small length of NNs ($L \sim 3\ \mu m$). This suggests that the NN arrays exhibit high absorption efficiency with minimal reflectance. In addition, patterned growth of Ge NNs can be readily achieved on substrates by patterning the Ni thin film regions prior to the growth, further depicting the catalytic role of Ni particles in the growth of the NNs (Supporting Information, Figure S3).

Reflectance measurements were performed to characterize the optical properties of Ge NN arrays. For this study, Ge

DOI: 10.1021/nl903366z | Nano Lett. 2010, 10, 520-523

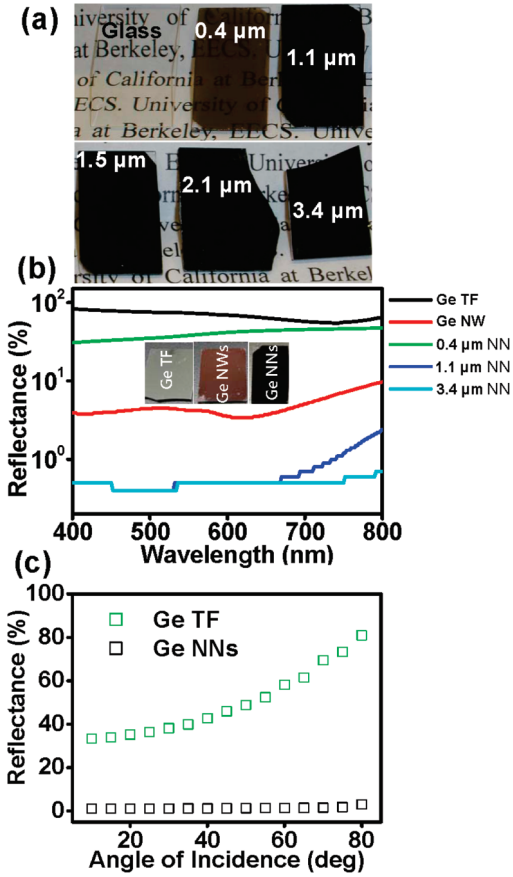

FIGURE 4. Reflectance studies of Ge NN arrays. (a) Optical images of Ge NNs with different lengths grown on glass substrates, demonstrating the visually black appearance for $L \geq 1.1$ μm. (b) The reflectance spectra of Ge TF, Ge NWs ($d \sim 30$ nm, $L \sim 20$ μm), and Ge NNs with different lengths. The inset shows the optical images of three representative substrates. (c) The angular dependent reflectance measurements at 780 nm for Ge TF and Ge NNs ($L \sim 1.1$ μm).

NNs were grown on transparent glass substrates. The corresponding optical images of Ge NN arrays with different lengths ($L = 0.4-3.4$ μm) are shown in Figure 4a. As evident, the substrates are completely opaque for NN lengths >1 μm with a black visual appearance. Figure 4b shows the reflectance at normal incidence versus wavelength for Ge NN arrays with different lengths as well as Au-catalyzed Ge NW arrays ($d \sim 30$ nm, $L \sim 20$ μm) and a Ge TF (~ 1 μm thick) substrate. When comparing the substrates with NNs to the TF, it is clear that a drastic reduction of reflectance occurs for NN length >1 μm. Beyond this length, the NN arrays exhibit a reflectance of <1 % for all wavelengths. In contrast, Ge NWs of all lengths, even as high as ~ 20 μm, exhibited a reflectance of 2−10%, inferior to the NN arrays. As compared to the previously published works in the literature, black Ge produced by etching has been shown to have a reflectance of ~ 3 %.[11] The remarkably low reflectance of Ge NN arrays can be attributed to (i) the cone-shaped feature of the structures with ultrasharp (~ 4 nm) tips and (ii) their near vertical orientation arising from their high surface density as enabled by the Ni catalytic growth. Specifically, Ge NNs with $L > 1.1$ μm, exhibit ~ 10 and ~ 100 times reduction in reflectance as compared to Ge NWs and TF samples, respectively (Figure 4b). The optical images of Ge TF, NWs ($d \sim 30$ nm, $L \sim 20$ μm) and NNs ($L \sim 1.1$ μm) substrates also clearly show the drastic reflectance suppression for NNs as compared to both NWs and TF (Figure 4b). For instance, the Ge TF substrate exhibits a shiny surface while the Ge NW arrays exhibit a brown color. This is in distinct contrast to the NN samples that exhibit a black visual appearance. To further characterize the antireflective properties, angular dependent reflectance measurements were performed on the Ge NN arrays (Figure 4c). The reflectance spectra of the TF and 1.1 μm NN array with incident angle varied from ~ 10 to 85 degrees was collected by using a diode laser with a wavelength of 780 nm as the light source. This angular dependent measurement shows that Ge NN array exhibits minimal reflectance, even at high incident angles.

The observed reflectance behavior can be explained by using the concept of effective refractive index, which is defined as the weighted average of the refractive index of air and Ge by area. This concept of gradual refractive index has been theoretically suggested to explain the low reflectance observed from moth eyes[12] and has been experimentally demonstrated by several research groups with tapered or conical-shaped vertical structures.[2] Similarly in our study, the large Fresnel reflection observed on planar Ge surface due to the large refractive index mismatch between the air ($n = 1$) and Ge ($n = 5.4$ at 633 nm) has been significantly reduced through a smooth transition of the refractive index from the ultrathin tip to the base of the tapered Ge NN near-vertical arrays. This smooth transition of refractive index is more efficient than the stepwise graded refractive index in multilayer structures fabricated by complicated procedures.[13] In addition, the conical-shaped vertical structures have been known to have advantages over multilayer antireflectors in terms of broad range of spectral bandwidths and incident angles.[2,13] This causes the NN arrays with ultrasharp tips to behave as an excellent antireflective coating.

Another important materials property for a number of optical and optoelectronic applications is the band gap. To

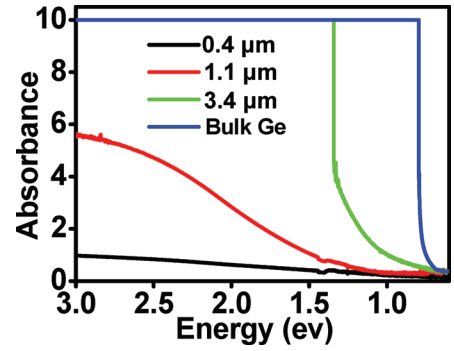

FIGURE 5. The absorption spectra of bulk Ge and Ge NN arrays with the lengths from 0.4 to 3.4 μm.

DOI: 10.1021/nl903366z | *Nano Lett.* **2010,** *10,* 520-523

obtain the effective band gap of Ge NN arrays, optical absorption spectroscopy was performed for NN arrays with lengths from 0.4 to 3.4 μm (Figure 5). As evident from the absorption spectra, Ge NN arrays with $L \sim 3.4$ μm nearly fully absorb the light for >1.2 eV, therefore, exhibiting a high absorption coefficient. The linear extrapolation to zero from $\alpha(E)^{1/2}$ as a function of photon energy yields an effective bandgap of $E_g \sim 1$ eV for Ge NNs. This band gap is larger than that of bulk crystalline Ge (~0.6 eV) but close to that of the amorphous Ge (~1.1 eV). The observed $E_g \sim 1$ eV for Ge NNs is attributed to the combination of amorphous Ge outershell and the quantum size-effects due to the ultrathin (~4 nm) crystalline core since the exciton Bohr radius of Ge is 17.7 nm.[14] In the future, further detailed characterization is needed to more clearly elucidate the observed band gap shift. From a practical point of view, an advantage of this bandgap shift lies in the potential use of Ge NNs as an absorber material for solar cell applications, more closely matching the solar spectrum peak. The combination of larger E_g, low reflectance, and high absorption efficiency may allow for a greater portion of solar energy to be converted into electrical energy, while keeping the overall materials thickness rather small. Since Ge NNs can be directly grown on plastic and rubber substrates, exploration of mechanically flexible photovoltaics may be feasible. Furthermore, Ge NNs are a promising material system for photodetectors, potentially exhibiting high detection sensitivity.

In summary, we report the growth of quasi-vertical Ge amorphous/crystalline core−shell nanoneedles by using Ni thin films as the catalyst via the VSS growth mechanism. The NNs exhibit a tapered structure with an average tip diameter as small as ~4 nm. By varying the growth temperature and pressure, the morphology and structure can be readily modified. The 3D structural configuration of Ge NNs results in superior antireflective properties due to the gradual reduction of the effective refractive index from the tip to the base of the highly dense NN arrays with ultrasharp tips. Because of the low reflectance and high optical absorption efficiency of the NN arrays, along with the ability to directly grow the material on low temperature substrates, various optoelectronics applications based on the reported black Ge may be envisioned in the future.

Acknowledgment. This work was supported by MARCO/MSD, Intel Corporation, NSF COINS, and Berkeley Sensor and Actuator Center. The nanowire synthesis part of this project was supported by a Laboratory Directed Research and Development grant from Lawrence Berkeley National Laboratory. N.M. and R.K. acknowledge NDSEG and NSF graduate fellowships, respectively.

Supporting Information Available. EDS quantitative analysis; XRD spectrum; selective growth of Ge NNs from patterned substrates. This material is available free of charge via the Internet at http://pubs.acs.org.

REFERENCES AND NOTES

(1) (a) Nelson, J. *The physics of solar cells*; Imperial College Press: London, **2003**. (b) Fahrenbruch, A. L.; Bube, R. H. *Fundamentals of Solar Cells: Photovoltaic Solar Energy Conversion*; Academic Press, Inc: New York, **1983**. (c) Spurgeon, J. M.; Atwater, H. A.; Lewis, N. S. *J. Phys. Chem. C* **2008**, *112*, 6186. (d) Fan, Z.; Razavi, H.; Do, J.-W.; Moriwaki, A.; Ergen, O.; Chueh, Y.-L.; Leu, P. W.; Ho, J. C.; Takahashi, T.; Reichertz, L. A.; Neale, S.; Yu, K.; Wu, M.; Ager, J. W.; Javey, A. *Nat. Mater.* **2009**, *8*, 648. (e) Lieber, C. M.; Wang, Z. L. *MRS Bull.* **2007**, *32*, 99.

(2) (a) Clapham, P. B.; Hutley, M. C. *Nature* **1973**, *244*, 281. (b) Huang, Y.-F.; Chattopadhyay, S.; Jen, Y.-J.; Peng, C.-Y.; Liu, T.-A.; Hsu, Y.-K.; Pan, C.-L.; Lo, H.-C.; Hsu, C.-H.; Chang, Y.-H.; Lee, C.-S.; Chen, K.-H.; Chen, L.-C. *Nat. Nanotechnol.* **2007**, *2*, 770. (c) Chen, Q.; Hubbard, G.; Shields, P. A.; Liu, C.; Allsopp, D. W. E.; Wang, W. N.; Abbott, S. *Appl. Phys. Lett.* **2009**, *94*, 263118. (d) Zhu, J.; Yu, Z.; Burkhard, G. F.; Hsu, C. M.; Connor, S. T.; Xu, Y.; Wang, Q.; McGehee, M.; Fan, S.; Cui, Y. *Nano Lett.* **2009**, *9*, 279.

(3) (a) Halbwax, M.; Sarnet, T.; Delaporte, Ph.; Sentis, M.; Etienne, H.; Torregrosa, F.; Vervisch, V.; Perichaud, I.; Martinuzzi, S. *Thin Solid Films* **2008**, *516*, 2791. (b) Shen, M.; Crouch, C. H.; Carey, J. E.; Younkin, R. J.; Mazur, E.; Sheehy, M. A.; Friend, C. M. *Appl. Phys. Lett.* **2003**, *82*, 1715. (c) Her, T.; Finlay, R. J.; Wu, C.; Deliwala, S.; Mazur, E. *Appl. Phys. Lett.* **1998**, *73*, 1673.

(4) (a) Ho, W. S.; Dai, Y.-H.; Deng, Y.; Lin, C.-H.; Chen, Y.-Y.; Lee, C.-H.; Liu, C. W. *Appl. Phys. Lett.* **2009**, *94*, 261107. (b) Tang, L.; Kocabas, S. E.; Latif, S.; Okayay, A. K.; Ly-Gagnon, D. S.; Saraswat, K. C.; Miller, D. A. B. *Nat. Photonics* **2008**, *2*, 226. (c) Zhu, J.; Dalal, V. L.; Ring, M. A.; Gutierrez, J. J.; Cohen, J. D. *J. Non-Cryst. Solids* **2004**, *338*, 651. (d) Krübler, W. *Appl. Phys. A* **1991**, *53*, 54.

(5) Wagner, R. S.; Ellis, W. C. *Appl. Phys. Lett.* **1964**, *4*, 89.

(6) Persson, A. L.; Larsson, M. W.; Stenstrom, S.; Ohlsson, B. J.; Sameulson, L.; Wallenberg, L. R. *Nat. Mater.* **2004**, *3*, 677.

(7) Nash, A.; Nash, P. *Bull. Alloy Phase Diagrams* **1987**, *8*, 255.

(8) Woo, R. L.; Gao, L.; Goel, N.; Hudait, M.; Wang, K. L.; Kodambaka, S.; Hicks, R. F. *Nano Lett.* **2009**, *9*, 2207.

(9) (a) Wang, D.; Tu, R.; Zhang, L.; Dai, H. *Angew. Chem., Int. Ed.* **2005**, *44*, 2925. (b) Hannon, J. B.; Kodambaka, S.; Ross, F. M.; Tromp, R. M. *Nature* **2006**, *440*, 69. (c) Kawashima, T.; Mizutani, T.; Nakagawa, T.; Torii, H.; Saitoh, T.; Komori, K.; Fujii, M. *Nano Lett.* **2008**, *8*, 362. (d) Lensch-Falk, J.; Hemesath, E. R.; Lopez, F. J.; Lauhon, L. J. *J. Am. Chem. Soc.* **2007**, *129*, 10670. (e) Kang, K.; Kim, D. A.; Lee, H. S.; Kim, C. J.; Yang, J. E.; Jo, M. H. *Adv. Mater.* **2008**, *20*, 4684.

(10) Tian, B.; Kempa, T. J.; Lieber, C. M. *Chem. Soc. Rev.* **2009**, *38*, 16.

(11) Gilbert, I. R.; Messier, R.; Roy, R. *Thin Solid Films* **1978**, *54*, 2.

(12) Bernhard, C. G. *Endeavour* **1967**, *26*, 79.

(13) Kuo, M.-L.; Poxson, D. J.; Kim, Y. S.; Mont, F. W.; Kim, J. K.; Schubert, E. F.; Lin, S.-Y. *Opt. Lett.* **2008**, *33*, 2527.

(14) Madelung, O. *Semiconductors: Data Handbook*, 3rd ed.; Springer-Verlag: Berlin, 2004.

DOI: 10.1021/nl903366z | *Nano Lett.* **2010,** *10,* 520-523